Fuel/Time Optimal Control of Flexible Space Structures: A Frequency Domain Approach

ROLF HARTMANN
TARUNRAJ SINGH
Department of Mechanical and Aerospace Engineering, State University of New York at Buffalo, Buffalo, NY, 14260, USA

(Received 6 March 1997; accepted 3 December 1997)

Abstract: This paper considers the design of open-loop fuel/time optimal controllers for flexible space structures using a frequency domain approach. The control system consists of a time-delay filter whose output signal is the optimal control profile when it is subject to a step input. A constrained parameter optimization problem is formulated to minimize a weighted combination of fuel consumed and total maneuver time for a rest-to-rest maneuver. The parameters to be optimized for are the delays of a time-delay filter. The number of switches of the fuel/time optimal control profile is shown to be a function not only of number of flexible modes but also of the weighting parameter, which is illustrated via numerical examples.

Key Words: Fuel/time optimal control, flexible space structures

1. INTRODUCTION

The design of optimal controllers for space structures has been extensively studied over the past decade. In most of these studies, the optimization objective has been the minimization of the maneuver time (Singh, Kabamba, and McClamroch, 1989; Singh and Vadali, 1994), the fuel consumed (Seywald et al., 1994; Silverberg and Redmond, 1993), or a weighted combination of both (Vander Velde and He, 1983; Hartmann, 1994). Since most large space structures are inherently restricted in weight, the structure is usually assumed to possess significant flexibility.

Recently, Seywald et al. (1994) investigated all possible control logics including singular controls in fuel optimal solutions for a rigid spacecraft reorientation problem. Silverberg and Redmond (1993) presented an exact numerical solution for fuel optimal reboost control problem for flexible spacecraft by using an adaptive Grid Bisection method. Singh, Kabamba, and McClamroch (1989) revealed the antisymmetric time property of time-optimal control profiles for rest-to-rest slewing maneuvers of flexible spacecrafts. They determined the switch times of an open-loop controller by solving a set of nonlinear algebraic equations.

The weighted fuel/time optimal control problem has been investigated with considerably less attention even though it is characterized by general applicability. Vander Velde and He (1983) presented a general approach for fuel/time optimal control of flexible structures with any number of flexible modes and any number of thrusters. The switching logic of the

Journal of Vibration and Control, 5: 795-817, 1999

feedback controller with "bang-off-bang" type profile is based on the gradient of the optimal cost function for any initial condition by decoupling the optimal control problem into separate subproblems for rigid body and flexible mode control. This technique has inherent difficulties in forcing the state to its final destination (origin of the state space). Lopes de Souza (1988) improved the final behavior of the control system by replacing the approximate solution of the flexible mode subproblem with the exact one. Wie et al. (1993) examined the robust fuel/time optimal control problem of undamped flexible structures with one and two flexible modes. They concluded that the "bang-off-bang" pulse sequences are the fuel/time optimal profiles. Recently, Singh and Vadali (1994) introduced a frequency domain approach to solve the time-optimal control problem. This technique was exploited to determine the closed-form solution of the fuel/time optimal control of a floating undamped oscillator (Singh, 1995).

The present work includes a frequency domain approach for the design of open-loop fuel/time optimal controllers for flexible space structures. The optimization addresses the minimization of a weighted combination of fuel consumed and final maneuver time. This problem is attractive since it covers the fuel-optimal and time-optimal cases in the limits of the weighting parameter α ($\alpha \to \infty$ and $\alpha \to 0$, respectively). The system to be controlled is represented by a linearized dynamic model with one rigid body mode and multiple flexible modes. The planar (single-axis) control maneuvers considered here are performed by using nonthrottleable on-off type actuators, which are commonly used for space structure control applications. Saturation limits of the actuator are taken into account by imposing magnitude constraints on the control signal. The open-loop control system consists of a time-delay filter, which generates an optimal control profile of the "bang-off-bang" type when subject to a step input. Such a design facilitates reformulation of the optimization problem as the optimization of the time delays of the filter. The parameter optimization problem is subject to constraint equations to satisfy the boundary conditions of the rest-to-rest maneuver and to prevent residual vibrations of the flexible modes, which are susceptible to being excited by the discontinuous nature of the control input.

The number of switches in the control profile not only is dependent on the number of flexible modes but also is a function of the weighting parameter. This leads to transition profiles for small values of the weighting parameter, which, in the limits of its valid range, is able to generate the time-optimal and the fuel/time optimal control profile (Singh, 1995). The points of transition of the control profiles correspond with the collapse of pulses in the control profile, whose exact determination is considered in this work.

The paper is organized as follows. The problem is formulated in Section 2. In Section 3, the control scheme and the corresponding design technique are introduced. Next, in Section 4, the constraints of the control optimization problem are stated, before the actual determination of the fuel/time optimal control profile is detailed in Section 5, which also includes remarks about optimality conditions. A simple numerical example illustrates the proposed design technique in Section 6. The number of switching points in the optimal control profile as a function of the weighting parameter leading to transition profiles is described in Section 7. The paper concludes with some observations in Section 8.

2. PROBLEM FORMULATION

The design of a controller for reorienting flexible space structures, which minimizes a performance index—a weighted combination of the maneuver time and fuel consumed—

is considered here. The final time is not prespecified, and the fuel flow rate is assumed to be proportional to the time the control is on. Thus, the design of fuel- and time-optimal control can be stated as the minimization of the performance index

$$J = \int_0^{t_f} (1 + \alpha |u|)\, dt, \tag{1}$$

where the performance index J is a summation of the final maneuver time t_f and the control fuel used. The weighting parameter, $\alpha > 0$, is chosen to indicate the relative importance of elapsed time and fuel expended.

The linearized dynamic model of a flexible space structure with one rigid body mode and flexible modes can be represented in the state space form:

$$\dot{\underline{x}} = A\underline{x} + Bu, \tag{2}$$

where $\underline{x} \in \Re^{2n+2}$ are the system states, A is the system matrix $(2n + 2) \times (2n + 2)$, and B is the control influence matrix. The problem considered here is a single input system, where B is a column matrix $(2n + 2) \times 1$ and the control input u is constrained such that

$$|u| \leq 1 \text{ for all } t \in [0, t_f]\,. \tag{3}$$

2.1. Boundary Conditions of the System

The flexible space structure considered in this paper is assumed to have no structural damping and can be represented by the vector differential equation of motion:

$$M\ddot{\underline{x}} + K\underline{x} = \underline{b}u, \tag{4}$$

where M is the mass matrix, K the stiffness matrix and $\underline{b}$ is the control influence vector, and $\underline{x}$ and u are the generalized coordinates and the scalar control input, respectively.

The boundary conditions for a rest-to-rest maneuver, which indicates no residual vibrations, are

$$\underline{x}(0) = 0, \underline{x}(t_f) = \underline{x}_f, \dot{\underline{x}}(0) = 0, \dot{\underline{x}}(t_f) = 0. \tag{5}$$

Decoupling the systems equation (equation 4) by a similarity transformation with the matrix of eigenvectors of the system Φ, we have

$$\begin{aligned} \ddot{\theta} &= \phi_0 u \\ \ddot{q}_i + \omega_i^2 q &= \phi_i u, \end{aligned} \tag{6}$$

where q_i is the ith modal coordinate, ω_i is the corresponding eigenfrequency ($i = 1$ to n), and θ is the rigid body coordinate. The new control influence vector is

$$\underline{\phi} = \begin{bmatrix} \phi_0 \\ \phi_1 \\ \cdots \\ \phi_n \end{bmatrix} = \Phi^{-1}\underline{b}.$$

The transformed rigid body and flexible mode boundary conditions are

$$q_i(0) = \dot{q}_i(0) = q_i(t_f) = \dot{q}_i(t_f) = 0 \tag{7}$$

$$\theta(0) = 0, \dot{\theta}(0) = 0, \theta(t_f) = \theta_f, \dot{\theta}(t_f) = 0, \tag{8}$$

where

$$\Phi^{-1}\underline{x}_f = \begin{bmatrix} \theta_f \\ 0 \\ \cdots \\ 0 \end{bmatrix}.$$

To ensure that the controller satisfies these boundary conditions (equations 7 and 8), we will derive appropriate constraint equations after we have parameterized the control profile.

3. PARAMETERIZATION OF THE CONTROL PROFILE

The design of the fuel/time optimal controller is reformulated as the design of a time-delay filter whose output is a bang-off-bang control profile after being subjected to a step-input signal (Figure 1). The amplitude of the filter signals is constrained to satisfy the control bounds (equation 3). Besides satisfying the actuator limits, the transfer function of the time-delay filter is required to cancel the poles of the system to prevent residual vibrations of the flexible modes at the final maneuver time (equation 7). The design of the time-delay filter also takes into account the boundary condition for the rigid body mode as stated in equation 8. We now solve a constrained parameter optimization problem where the parameters to be optimized for are the time delays of the filter that correspond to the switch times of the bang-off-bang control profile.

In previous works, the time-optimal control profile for undamped systems was noted to be antisymmetric about mid-maneuver time (Singh, 1989). As we assume no structural damping in our system, we also use a transfer function of an antisymmetric profile, which can be shown to cancel two poles at the origin of the s-plane. Furthermore, the antisymmetry of the control reduces the number of parameters to be optimized for.

While the optimization theory (Pontryagin's minimum principle) leads to bang-bang profile in time-optimal control, it results in a bang-off-bang profile in the fuel- and time-optimal cases. The intuitive justification for penalizing the fuel consumed for large values of the weighting parameter, α, leads to the assumption of a control structure with only positive pulses in the acceleration phase before mid-maneuver time and only negative pulses in the deceleration phase after mid-maneuver time, as also seen in Wie et al. (1993).

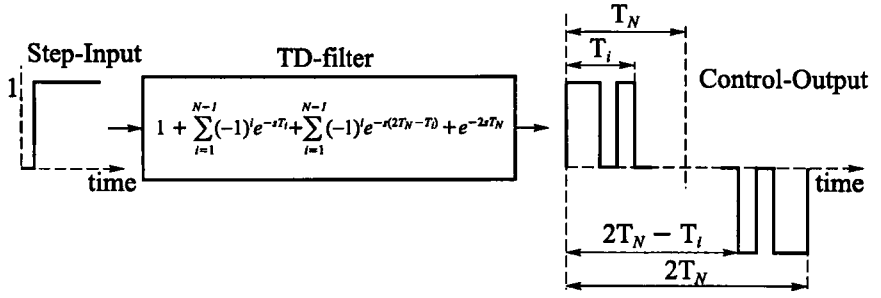

Figure 1. Time delay filter.

Thus, the bang-off-bang control input profile is expressed in the frequency domain as a summation of time-delayed step-inputs where the time delays correspond to the switch times of the control:

$$u = \frac{1}{s}\left(1 + \sum_{i=1}^{N-1}(-1)^i e^{-sT_i} + \sum_{i=1}^{N-1}(-1)^i e^{-s(2T_N - T_i)} + e^{-2sT_N}\right), \tag{9}$$

where T_N is the mid-maneuver time, $T_i (i = 1 \ldots N-1)$ are the switching times before mid-maneuver time, and $2T_N - T_i$ are the corresponding switching times after mid-maneuver time.

The transfer function of the time-delay filter consequently is

$$G(s) = 1 + \sum_{i=1}^{N-1}(-1)^i e^{-sT_i} + \sum_{i=1}^{N-1}(-1)^i e^{-s(2T_N - T_i)} + e^{-2sT_N}. \tag{10}$$

This transfer function has to satisfy all boundary conditions (equations 7 and 8), which can be achieved by canceling all poles of the system.

As will be illustrated in the following sections, the number of parameters to be determined, N, are not linearly related to the number of flexible modes n but are given as follows:

$$N = n + 1, \text{ for } n = 1, 3, 5, \ldots \text{ (odd number of flexible modes)}$$
$$N = n + 2, \text{ for } n = 0, 2, 4, \ldots \text{ (even number of flexible modes)}$$

This implies that the same number of switches are required for the system with even number of modes n and the system with odd number of modes $n + 1$. The case-dependent relationship between number of modes and number of switches is inherent for fuel- and time-optimal control and will be discussed later.

4. CONSTRAINTS OF FUEL/TIME OPTIMAL CONTROL PROBLEM

4.1. Rigid Body Constraint

The fuel/time optimal controller has to satisfy the rest-to-rest constraint of the rigid body mode. To derive the rigid body constraint in terms of the unknown parameters, we consider the Laplace transformed decoupled rigid-body mode equation of motion with the parameterized control input:

$$\begin{aligned} s^2\theta(s) &= \phi_0 u \\ &= \phi_0 \frac{1}{s}\left(1 + \sum_{i=1}^{N-1}(-1)^i e^{-sT_i} + \sum_{i=1}^{N-1}(-1)^i e^{-s(2T_N - T_i)} + e^{-2sT_N}\right). \end{aligned} \tag{11}$$

Evaluating the inverse Laplace transformation of equation (11) and equating the rigid body mode θ at final time $t_f = 2T_N$ to θ_{final} leads to the following constraint equation:

$$\begin{aligned} \theta(t_{final}) &= \theta(2T_N) \\ &= \phi_0\left(2T_N^2 + \sum_{i=1}^{N-1}(-1)^i \frac{(2T_N - T_i)^2}{2} + \sum_{i=1}^{N-1}(-1)^i \frac{T_i^2}{2}\right) = \theta_{final}. \end{aligned} \tag{12}$$

4.2. Pole Cancellation Constraint

The transfer function (equation 10) has to cancel all poles of the system to avoid residual vibrations at the final time as expressed in the boundary conditions for the flexible modes (equation 7). The undamped system we consider has two rigid body poles at the origin of the s-plane and n complex conjugate poles along the imaginary-axis. The transfer function $G(s)$ has two zeros at the origin $(s = 0)$, as

$$G(s = 0) = 0 \text{ and } \left.\frac{dG}{ds}\right|_{s=0} = 0,$$

therefore canceling the two rigid body poles, and thus the velocity constraint of the rigid body mode, at final time, is automatically satisfied.

As all other flexible mode poles of the system at $s_k = \pm j\omega_k\,(k = 1 \ldots n)$ are required to be canceled to satisfy the final time-flexible mode constraint (equation 7), we force the transfer function zeros to coincide with the location of the system poles by deriving appropriate constraint equations.

The imaginary poles $s_k = \pm j\omega_k$ are canceled by $G(s)$ if

$$G(s_k) = 0. \tag{13}$$

Substituting $s_k = j\omega_k$ in equation (13) and equating both real and imaginary parts to zero, leads to

$$1 + \sum_{i=1}^{N-1} (-1)^i \cos \omega_k T_i + \sum_{i=1}^{N-1} (-1)^i \cos \omega_k (2T_N - T_i) + \cos 2\omega_k T_N = 0 \tag{14}$$

$$\sum_{i=1}^{N-1} (-1)^i \sin \omega_k T_i + \sum_{i=1}^{N-1} (-1)^i \sin(\omega_k (2T_N - T_i)) + \sin 2\omega_k T_N = 0. \tag{15}$$

These equations can be rewritten after algebraic manipulations as

$$2 \cos (\omega_k T_N) \left\{ \sum_{i=1}^{N-1} (-1)^i \cos \omega_k (T_N - T_i) + \cos \omega_k T_N \right\} = 0 \tag{16}$$

$$2 \sin (\omega_k T_N) \left\{ \sum_{i=1}^{N-1} (-1)^i \cos \omega_k (T_N - T_i) + \cos \omega_k T_N \right\} = 0. \tag{17}$$

Satisfaction of the equation

$$\sum_{i=1}^{N-1} (-1)^i \cos \omega_k (T_N - T_i) + \cos \omega_k T_N = 0, \; k = 1 \ldots n \tag{18}$$

implies the satisfaction of equations (16) and (17) and leads to n constraint equations. We now have $n+1$ constraints in N parameters, where N is always greater than or equal to $n+1$.

5. DETERMINATION OF THE FUEL/TIME OPTIMAL CONTROL

The fuel/time optimal control profile can be determined by solving the constrained parameter-optimization problem. The performance index to be minimized (equation 1) can be rewritten in terms of the unknown parameters as

$$J = 2T_N + \alpha \left(2 \sum_{i=1}^{N-1} (-1)^{i+1} T_i \right). \tag{19}$$

The parameter optimization problem can be stated as the minimization of J subject to the constraints:

$$\sum_{i=1}^{N-1} (-1)^i \cos \omega_k (T_N - T_i) + \cos \omega_k T_N = 0, \; k = 1, 2 \ldots, n, \tag{20}$$

$$\frac{\phi_0}{\theta_{final}} \left(2T_N^2 + \sum_{i=1}^{N-1} (-1)^i \frac{(2T_N - T_i)^2}{2} + \sum_{i=1}^{N-1} (-1)^i \frac{T_i^2}{2} \right) - 1 = 0 \tag{21}$$

and

$$T_N > T_{N-1} > \ldots > T_2 > T_1 > 0, \tag{22}$$

where

$$\begin{aligned} N &= n+1, \text{ for odd number of flexible modes} \\ N &= n+2, \text{ for even number of flexible modes.} \end{aligned}$$

A sequential quadratic programming algorithm with user-supplied gradients of the performance index (19) and the constraints (20-22) is used to solve the constrained optimization problem.

5.1. Necessary Conditions for Optimality

The necessary conditions for the optimality of the fuel/time optimal controller are listed below. For the fuel- and time-optimal control problem considered here, the Hamiltonian H is

$$H = 1 + \alpha |u| + \underline{\lambda}^T (A\underline{x} + B\underline{u}), \tag{23}$$

where $\underline{\lambda} \in \Re^{2n+2}$ is the costate vector. u^* is called an optimal control if the following set of necessary conditions is satisfied:

$$\frac{\partial H}{\partial \underline{\lambda}} = \dot{\underline{x}}^* = A\underline{x}^* + B\underline{u}^*, \forall t \in [0, t_f] \text{ (state eqn)} \tag{24}$$

$$\frac{\partial H}{\partial \underline{x}} = -\dot{\underline{\lambda}}^* = A^T \lambda^*, \forall t \in [0, t_f] \text{ (costate eqn)} \tag{25}$$

$$H(\underline{x}^*, \underline{u}^*, \underline{\lambda}^*) \leq H(\underline{x}^*, \underline{u}, \lambda^*), \forall t \in [0, t_f] \tag{26}$$

$$H(\underline{x}^*, \underline{u}^*, \lambda^*) = 1 + \alpha |u^*| + \underline{\lambda}^{*T} (A\underline{x}^* + B\underline{u}^*) = 0, \forall t \in [0, t_f]. \tag{27}$$

Equation (27) is a necessary condition since the final time t_f is free and H does not contain t explicitly (Athans and Falb, 1966; Kirk, 1970). Pontryagin's minimum principle is expressed by equation (26) and indicates that the optimal control u^* has to minimize the Hamiltonian H along the optimal trajectory. The minimum principle is used, since $\frac{\partial H}{\partial u} = 0$ cannot be determined analytically. With the knowledge that the optimal control minimizes the Hamiltonian, we need to consider only those terms of the Hamiltonian that are functions of u:

$$H'(u,\underline{\lambda}) = \begin{cases} (\underline{\lambda}^T B + \alpha)u, u \geq 0 \\ (\underline{\lambda}^T B - \alpha)u, u < 0 \end{cases}.$$

With the control constraint $| u | \leq 1$, the switching logic

$$\begin{aligned} u &= +1, \text{ if } \underline{\lambda}^T B < -\alpha \\ u &= -1, \text{ if } \underline{\lambda}^T B > \alpha \\ u &= 0, \text{ if } -\alpha < \underline{\lambda}^T B < \alpha \end{aligned}$$

minimizes the Hamiltonian. Thus, a switch in $u^*(t)$ occurs if the switching function $\underline{\lambda}^{*T}(t)B$ crosses the horizontal lines with ordinate intercept of α or $-\alpha$ at the switching times $T = T_1, T_2, \ldots, T_{N-1}$. With the definition of the deadzone function:

$$dez(z) = \begin{cases} -1, z < -1 \\ 0, |z| \leq 1 \\ 1, z > 1 \end{cases}.$$

$u^*(t)$ can be expressed as follows:

$$u^*(t) = -dez\left(\frac{\underline{\lambda}^{*T}(t)B}{\alpha}\right) = -dez\left(\frac{B^T\underline{\lambda}^*(t)}{\alpha}\right). \tag{28}$$

Therefore, the optimal control $u^*(t)$ can be uniquely specified as a function of the switching function $B^T\underline{\lambda}^*(t)$, if the switching function has no singular interval. Hartmann (1994) has shown that the problem considered is normal, which precludes singular intervals.

5.2. Solving for Optimal Control

By excluding singular intervals in the switching function as shown in Hartmann (1994) we assume normality of the problem and thus the optimal control $u^*(t)$ is determined by the optimal costates $\underline{\lambda}^*(t)$. The costates are given by the solution of equation (25), which is

$$\underline{\lambda}^*(t) = e^{-A^T t}\underline{\lambda}^*(0). \tag{29}$$

Thus, solving for $\underline{\lambda}^*(0)$ also determines the optimal control profile $u^*(t)$. To determine $\underline{\lambda}^*(0) \in \Re^{2n+2}$, we need a set of $2n+2$ independent equations.

From the switching logic (equation 28) we know the exact value of the switching function at the $(2N-2)$-switch times $T_s = T_1, \ldots, T_{N-1}, 2T_N - T_{N-1}, \ldots, 2T_N - T$:

$$\frac{\underline{\lambda}^{*T}(T_s)B}{\alpha} = \pm 1, \text{ if } u^*(T_s) \mp 1. \tag{30}$$

Substituting equation (29) in equation (30), we obtain equations that have to be satisfied at every switch time:

$$
\begin{aligned}
B^T e^{-A^T T_s}\ \underline{\lambda}^*(0) &= -\alpha\,, \text{ for } T_s = T_1, \ldots, T_{N-1} \\
B^T e^{-A^T T_s}\ \underline{\lambda}^*(0) &= \alpha\,, \text{ for } T_s = 2T_N - T_{N-1}, \ldots, 2T_N - T_1.
\end{aligned} \tag{31}
$$

In the case of an even number of flexible modes, $N = n + 2$ and equation (31) provide $2n + 2$ equations that are sufficient to compute $\underline{\lambda}^*(0) \in \Re^{2n+2}$. But we will include another optimality condition and a costate-characteristic to obtain two more linearly independent equations. This allows us to have a sufficient set of independent equations for determining $\underline{\lambda}^*(0)$ even in the case of an odd number of flexible modes where $N = n + 1$.

As stated previously, the Hamiltonian H is not explicitly a function of time and the final time in the fuel- and time-optimal problem is free, thus the necessary condition (equation 27) of the Hamiltonian being equal to zero for $\forall t \in [0, t_f]$ gives us:

$$
H(\underline{x}^*(0), \underline{u}^*(0), \underline{\lambda}^*(0)) = 1 + \alpha + \underline{\lambda}^{*T}(0)B = 0
$$

or

$$
B^T \underline{\lambda}^*(0) = -1 - \alpha\,. \tag{32}
$$

Furthermore, it was shown in Hartmann (1994) that for our problem the costates corresponding to every state representing velocity are equal to zero at mid-maneuver time T_N and thus the switching function at mid-maneuver time is

$$
\underline{\lambda}^T(T_N)B = 0. \tag{33}
$$

We can express equation (33) in terms of $\underline{\lambda}^*(0)$ by

$$
B^T e^{-A^T T_N}\ \underline{\lambda}^*(0) = 0. \tag{34}
$$

Equations (32) and (34) provide us with two linearly independent equations, which enables us to solve for $\underline{\lambda}^*(0)$ even in the case of odd number of flexible modes. Thus, $\underline{\lambda}^*(0)$ can be determined by solving the matrix equation (equation 35), which combines equations (31), (32), and (34):

$$
\begin{bmatrix}
B^T e^{-A^T T_1} \\
B^T e^{-A^T T_2} \\
\cdots \\
B^T e^{-A^T (2T_N - T_2)} \\
B^T e^{-A^T (2T_N - T_1)} \\
B^T \\
B^T e^{-A^T T_N}
\end{bmatrix}
\underline{\lambda}^*(0) = P\underline{\lambda}^*(0) =
\begin{bmatrix}
-\alpha \\ -\alpha \\ \cdots \\ \alpha \\ \alpha \\ -1-\alpha \\ 0
\end{bmatrix}, \tag{35}
$$

where P is a square matrix for the case with an odd number of flexible modes $(N = n + 1)$.

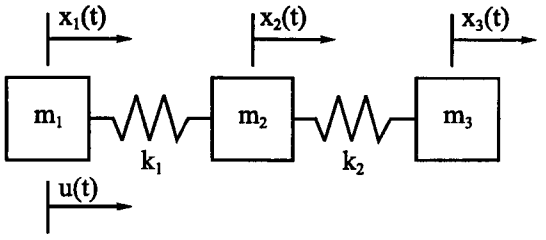

Figure 2. Three-mass-spring system.

After substituting the parameters $T_1, T_2, \ldots, T_N$ obtained from the parameter optimization algorithm into the matrix equation (35), we can solve for $\underline{\lambda}^*(0)$, and therefore the optimal control profile, by the switching logic stated in equation (28). If the control profile $u(t)$ determined by the optimized parameters $T_1, T_2, \ldots, T_N$ switches exactly at the switching times of the optimal control $u^*(t)$ (equation 28),

$$u(t) = u^*(t),$$

the (necessary) conditions for optimality are satisfied and the control can be considered to be optimal.

6. NUMERICAL EXAMPLE

Singh (1995) has solved the fuel- and time-optimal control problem for the benchmark two-mass-spring system in closed form. Since a system with an increased complexity cannot be solved exactly, we consider the fuel- and time-optimal control problem of a three-mass-spring system to demonstrate the feasibility of the proposed design technique.

6.1. Three-Mass-Spring System

The system dynamic is characterized by the masses m_1, m_2, m_3 and the stiffness of the springs k_1, k_2 (Figure 2). The control $u(t)$ is applied on the first mass with the objective of controlling the displacement of all masses of the system.

The matrix equation of motion for this system is

$$\begin{bmatrix} m_1 & 0 & 0 \\ 0 & m_2 & 0 \\ 0 & 0 & m_3 \end{bmatrix} \begin{bmatrix} \ddot{x}_1 \\ \ddot{x}_2 \\ \ddot{x}_3 \end{bmatrix} + \begin{bmatrix} k_1 & -k_1 & 0 \\ -k_1 & k_1 + k_2 & -k_2 \\ 0 & -k_2 & k_2 \end{bmatrix} \begin{bmatrix} x_1 \\ x_2 \\ x_3 \end{bmatrix} = \begin{bmatrix} 1 \\ 0 \\ 0 \end{bmatrix} u, \qquad (36)$$

with the boundary conditions for a rest-to-rest maneuver being

$$\underline{x}(0) = 0, \underline{x}(t_f) = \underline{x}_f, \dot{\underline{x}}(0) = 0, \dot{\underline{x}}(t_f) = 0. \tag{37}$$

Decoupling equation (36) with the matrix of eigenvectors Φ leads to

$$\begin{bmatrix} 1 & 0 & 0 \\ 0 & 1 & 0 \\ 0 & 0 & 1 \end{bmatrix} \begin{bmatrix} \ddot{\theta} \\ \ddot{q}_1 \\ \ddot{q}_2 \end{bmatrix} + \begin{bmatrix} 0 & 0 & 0 \\ 0 & \omega_1^2 & 0 \\ 0 & 0 & \omega_2^2 \end{bmatrix} \begin{bmatrix} \theta \\ q_1 \\ q_2 \end{bmatrix} = \begin{bmatrix} \phi_0 \\ \phi_1 \\ \phi_2 \end{bmatrix} u, \tag{38}$$

where ω_1 and ω_2 are the eigenfrequencies of the system. The decoupled boundary conditions are

$$\underline{q}(0) = \dot{\underline{q}}(0) = \underline{q}(t_f) = \dot{\underline{q}}(t_f) = 0$$

$$\theta(0) = 0, \dot{\theta}(0) = 0, \theta(t_f) = \theta_f, \dot{\theta}(t_f) = 0. \tag{39}$$

Since we have an even number of flexible modes ($n = 2$), we need to determine $N = n + 2 = 4$ parameters for the corresponding fuel- and time-optimal control profile, which is determined by the transfer function of the time-delay filter

$$G(s) = 1 - e^{-sT_1} + e^{-sT_2} - e^{-sT_3} - e^{-s(2T_4 - T_3)} + e^{-s(2T_4 - T_2)} - e^{-s(2T_4 - T_1)} + e^{-2sT_4}. \tag{40}$$

The optimization problem is to minimize

$$J = 2T_4 + \alpha(2T_1 + 2(T_3 - T_2)), \tag{41}$$

subject to the constraint equations

$$-\cos\omega_1(T_4 - T_1) + \cos\omega_1(T_4 - T_2) - \cos\omega_1(T_4 - T_3) + \cos\omega_1 T_4 = 0, \tag{42}$$

$$-\cos\omega_2(T_4 - T_1) + \cos\omega_2(T_4 - T_2) - \cos\omega_2(T_4 - T_3) + \cos\omega_2 T_4 = 0, \tag{43}$$

$$\frac{\phi_0}{\theta_{final}} \left(2T_4^2 - \frac{(2T_4 - T_1)^2}{2} + \frac{(2T_4 - T_2)^2}{2} - \frac{(2T_4 - T_3)^2}{2} - \frac{T_1^2}{2} + \frac{T_2^2}{2} - \frac{T_3^2}{2} \right) - 1 = 0, \tag{44}$$

and

$$T_4 > T_3 > T_2 > T_1 > 0.$$

6.2. *Equivalent Rigid Model*

The fuel- and time-optimal control for a corresponding rigid model of the flexible structure can be solved analytically in closed form and serves as a reference to compare the results of the flexible system. Thus, the mass of the equivalent rigid model is identical with the total mass of the three-mass-spring system and its equation of motion is

$$\left(\sum_{i=1}^{3} m_i\right)\ddot{x} = u, \tag{45}$$

where x is the rigid body displacement and u the control input

$$u = \frac{1}{s}\left(1 - e^{-sT_1} - e^{-s(2T_2 - T_1)} + e^{-2sT_2}\right) \tag{46}$$

is parameterized in terms of the first switch time T_1 and the mid-maneuver time T_2. Solving equation (45) in terms of the parameterized control u, so as to satisfy the boundary conditions (equation 37), we have

$$T_2 = \frac{x_f \sum_{i=1}^{3} m_i + T_1^2}{2T_1}. \tag{47}$$

The performance index can be expressed in terms of T_1 as

$$J_r(T_1) = \frac{x_f \sum_{i=1}^{3} m_i}{T_1} + 2\alpha T_1. \tag{48}$$

The minimization of J_r is given by $\dfrac{dJ_r}{dT_1} = 0$, which leads to the optimized parameter

$$T_1^* = \sqrt{\frac{x_f \sum_{i=1}^{3} m_i}{2\alpha + 1}}. \tag{49}$$

The corresponding optimal performance index is

$$J_r^* = 2\sqrt{(2\alpha + 1)\, x_f \sum_{i=1}^{3} m_i}. \tag{50}$$

The variation of J_r^*, T_1^*, and $2T_2^*$ for the rigid model as a function of α are compared with the corresponding value for the flexible structure to exemplify the peculiarities of the optimal control solution for the flexible structure.

6.3. *Effects of Variation of* α

The effect of the weighting parameter α on the optimal control is studied next. We use the nominal values of the parameters with $m_1 = m_2 = m_3 = 1$ and $k_1 = k_2 = 1$ with

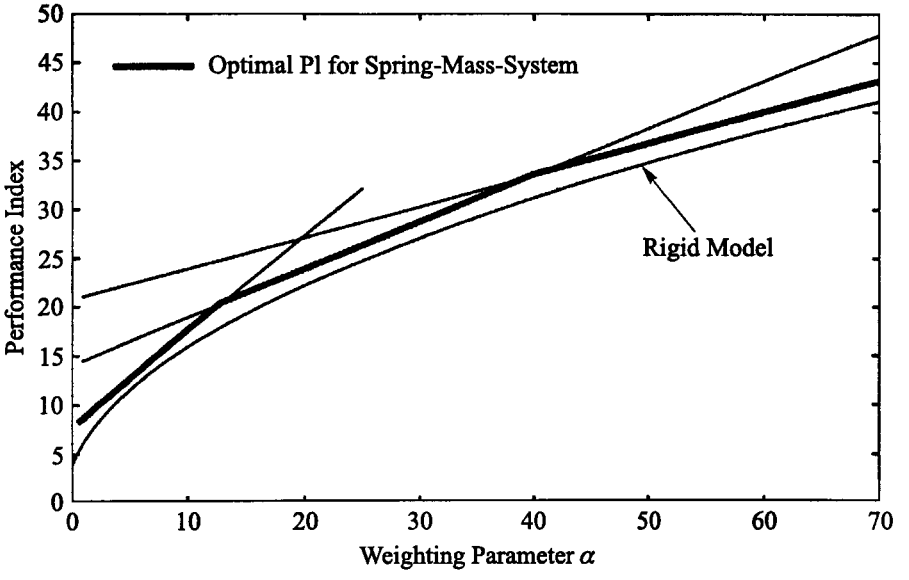

Figure 3. Performance index as a function of α.

appropriate units to obtain the variation of the optimal solution as a function of α. The corresponding eigenfrequencies are $\omega_1 = 1$, $\omega_2 = \sqrt{3}$, and for a rest-to-rest maneuver with $\underline{x}(t_f) = 1$, the quotient of the rigid body boundary constraint equation (equation 44) is

$$\frac{\phi_0}{\theta_{final}} = \frac{1}{3}.$$

Four parameters have to be solved in the previously described optimization problem with three constraint equations. The presence of trigonometric functions in the constraint equations results in multiple admissible solutions, all of which satisfy the constraint equations. Thus, the optimization algorithm converges to different solutions that are strongly dependent on the initial guess. To obtain the optimal solution, the results have to be filtered by the optimality conditions as described in 5.2. The variation of the optimal performance index as a function of α, $(\alpha > 1)$ is shown in Figure 3.

Each piecewise linear curve of the highlighted graph corresponds to the optimal control in a certain range of α. At the location of the discontinuities, the optimal solution jumps to another set of switching parameters as clearly shown in the variation of the final switch time as a function of α (Figure 4). The piecewise linear characteristic was also observed in the closed-form solution of the two-mass-spring system by Singh (1995) and can be attributed to the fact that the constraint equations are a function of trigonometric expressions leading to multiple optimal solutions. Generally, increasing α forces the fuel consumption to decrease due to shorter pulse width at the expense of the final maneuver time (Figures 4 and 5). Figure 3 illustrates that the optimal performance index of the flexible structure resides in the vicinity of the corresponding rigid structure.

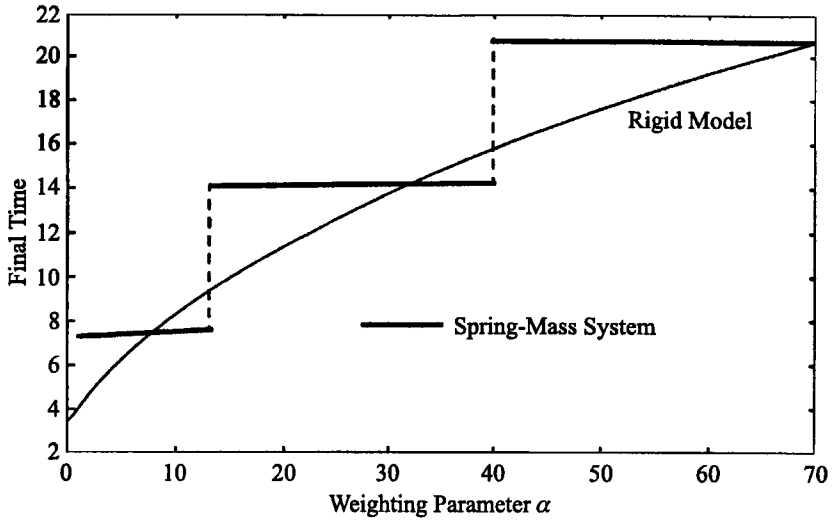

Figure 4. Final maneuver time as function of α.

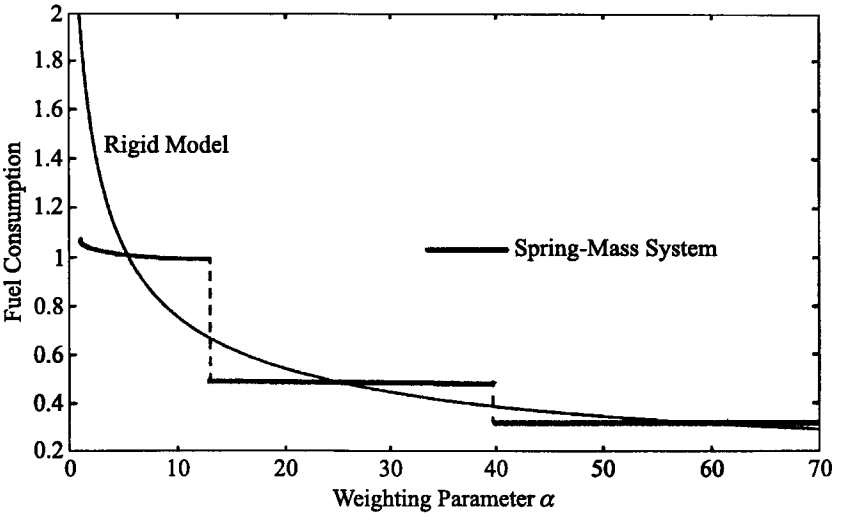

Figure 5. Fuel consumption as function of α.

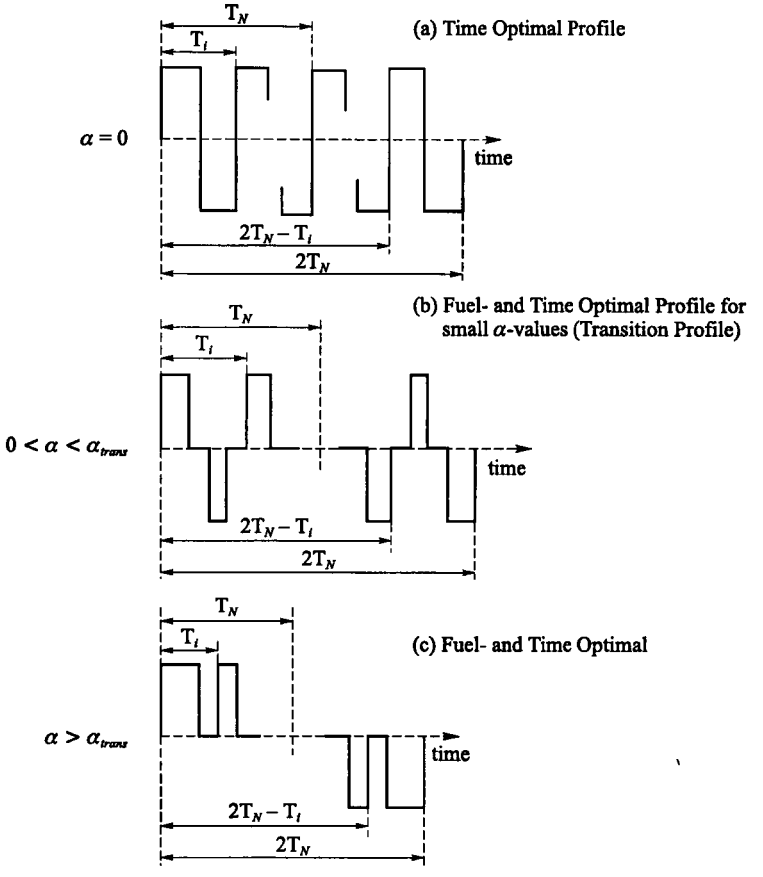

Figure 6. Transition from time-optimal to fuel/time optimal control.

For large values of α, the changes within the range of one set of optimal solutions become very small. Thus, the change in the performance index in this range is mainly caused by the variation of α itself.

7. TRANSITION PROFILE

7.1. Profile for Small Values of α

The fuel- and time-optimal control problem includes the time-optimal control case ($\alpha = 0$). The optimization theory (Pontryagin's minimum principle) establishes that the time-optimal control profile is of the "bang-bang" type as shown in Figure 6(a). Each switch in the bang-bang profile corresponds with the switching function changing signs ($\alpha = 0$). As soon as $\alpha > 0$, an interval exists between $+\alpha$ and $-\alpha$ in which the switching function requires the control to be zero. This forces the bang-bang into a bang-off-bang profile as shown in Figure 6(b). This transition profile is marked by negative (decelerating) pulses in the acceleration

phase ($t < T_N$) and positive (accelerating) pulses in the deceleration phase ($t > T_N$), which tend to collapse with an increasing α, which penalizes the fuel-consumption. The value of α corresponding to the collapse of these pulses is denoted with α_{trans} and determines the transition from the small α profile to the fuel- and time-optimal control profile as shown in Figure 6(c). In the limits $\alpha = 0$ and $\alpha = \alpha_{trans}$, the transition profile structure can generate both the time-optimal profile and the fuel- and time-optimal profile described in the previous section.

7.2. Number of Switching Points in the Fuel/Time Optimal Control Profile

The number of switch times, p, in the time-optimal profile is linearly dependent to the number of flexible modes n (Singh and Vadali, 1994) and is given by the relationship

$$p_{timeopt} = 2n + 1.$$

Since the antisymmetry of the time-optimal profile reduces the number of parameters N determining the profile structure, the relationship of the number of parameters to be solved, to the number of flexible modes is

$$N_{timeopt} = n + 1.$$

With $\alpha > 0$, every switch of the time-optimal profile leads to two switches of the transition profile, leading to

$$p_{trans} = 4n + 2 \text{ and } N_{trans} = 2n + 2,$$

where p_{trans} is the number of switches and N_{trans} the number of parameters to be determined in the transition profile. The bang-off-bang structure of the generated transition profile reveals n pulses, which collapse for $\alpha = \alpha_{trans}$ in the case of an even number of flexible modes, and $n + 1$ pulses collapse in the case of an odd number of flexible modes. Each collapsing pulse corresponds to the reduction of two parameters. The case-dependent number of collapsing pulses causes the resulting case-dependent number of parameters to be determined for the fuel- and time-optimal profile ($\alpha > \alpha_{trans}$) detailed in the previous section with

$$\begin{aligned} N &= n + 1, \text{ for } n = 1, 3, 5, \ldots \text{ (odd number of flexible modes)} \\ N &= n + 2, \text{ for } n = 0, 2, 4, \ldots \text{ (even number of flexible modes)} \end{aligned}$$

Thus, the structure of the transition profile changes due to increased penalization of fuel consumption with $\alpha > \alpha_{trans}$, which results in the collapse of all fuel-wasting pulses and leads to the case-dependent number of switch times in the fuel- and time-optimal control profile.

7.3. Determination of α_{trans}

The value of α_{trans} where the fuel- and time-optimal control profile for large α transforms into the transition profile for small α is determined by using the switching function $B^T\lambda(t)$

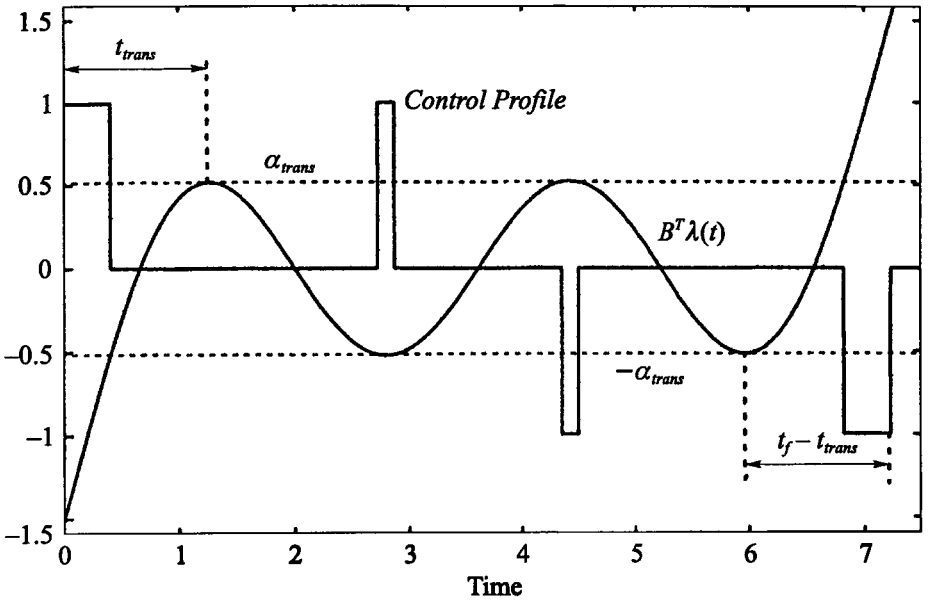

Figure 7. Large α control profile with $\alpha \approx \alpha_{trans}$.

corresponding to α_{trans}. This switching function tangentially touches the lines parallel to the abscissa with ordinate intercept value of α_{trans} at the time t_{trans} and the line with ordinate intercept value of $-\alpha_{trans}$ at $t_f - t_{trans}$, respectively, as shown in Figure 7. This leads to the following equations:

$$B^T\lambda\,(t_{trans}) = B^T e^{-A^T t_{trans}}\ \lambda\,(0) = \alpha_{trans} \tag{51}$$

$$\frac{d}{dt}(B^T\lambda\,(t))\bigg|_{t=t_{trans}} = -B^T A^T e^{-A^T t_{trans}}\ \lambda\,(0) = 0 \tag{52}$$

$$B^T\lambda\,(t_f - t_{trans}) = B^T e^{-A^T (t_f - t_{trans})}\ \lambda\,(0) = -\alpha_{trans} \tag{53}$$

$$\frac{d}{dt}(B^T\lambda\,(t))\bigg|_{t=t_f - t_{trans}} = -B^T A^T e^{-A^T (t_f - t_{trans})}\ \lambda\,(0) = 0 \tag{54}$$

To solve the nonlinear equations (51)-(54) for the two unknowns α_{trans} and t_{trans}, the corresponding switching function has to be evaluated. $\lambda\,(0)$, which determines the switching function, can be computed from the matrix equation (35) detailed in Section 5.2.

With $\underline{\lambda}(0) = P^{-1}\,[-\alpha\ -\alpha\ \ldots\,\alpha\,\alpha\ -1-\alpha\,0]^T$, the set of nonlinear equations can be written as

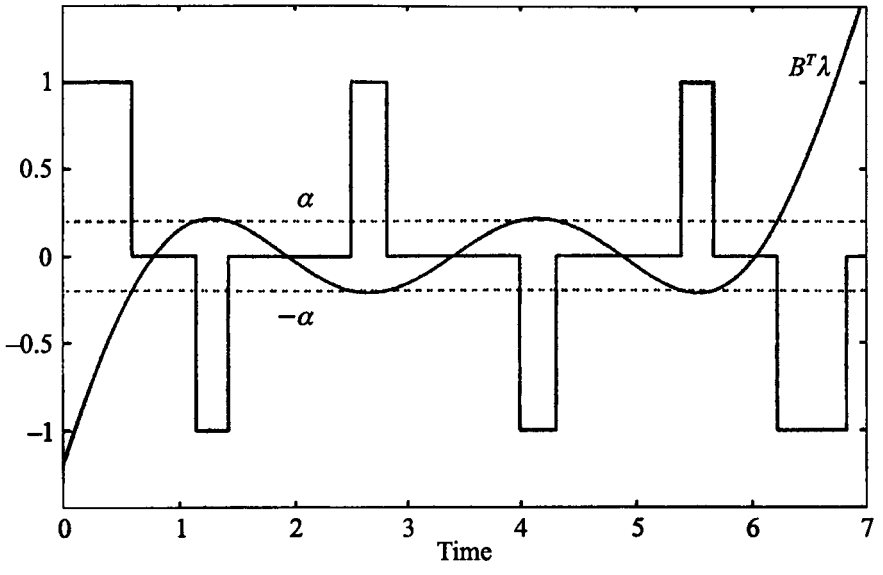

Figure 8. Small α profile for three-mass-spring system.

$$\begin{bmatrix} B^T e^{-A^T t_{trans}} \\ -B^T A^T e^{-A^T t_{trans}} \\ B^T e^{-A^T (t_f - t_{trans})} \\ -B^T e^{-A^T (t_f - t_{trans})} \end{bmatrix} P^{-1} [-\alpha_{trans} \quad -\alpha_{trans} \quad \cdots$$

$$\alpha_{trans} \; \alpha_{trans} \; -1-\alpha_{trans} \; 0]^T = \begin{bmatrix} \alpha_{trans} \\ 0 \\ -\alpha_{trans} \\ 0 \end{bmatrix}, \tag{55}$$

which can be solved for α_{trans} and t_{trans} by a nonlinear equation-solving algorithm. Due to the variation of $T_1, T_2, \ldots, T_N$ with α, the optimization algorithm has to be implemented into the nonlinear equation-solving algorithm to provide the equation solver with the appropriate values of $T_1, T_2, \ldots, T_N$ and P^{-1}, respectively.

7.4. Numerical Examples of α_{trans}

The effect of the mechanical properties of the flexible structure on α_{trans} is studied for the three-mass-spring case, where only one transition switch point and one additional pulse-pair exist (Figure 8).

Increasing both stiffness-coefficients, k_1 and k_2, simultaneously by a stiffness factor, changes the frequencies of the vibratory modes proportionally. The effect of the variation

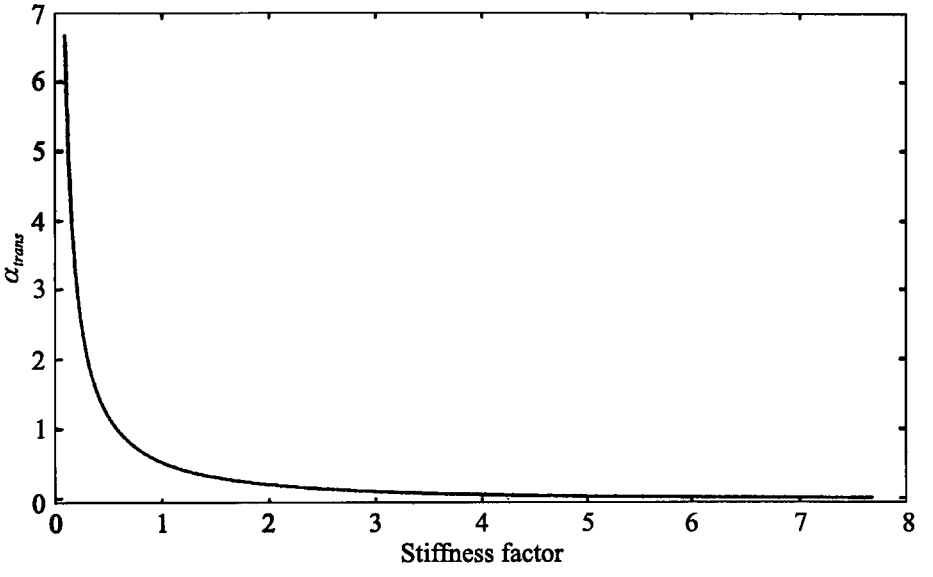

Figure 9. Variation of α_{trans} versus stiffness factor.

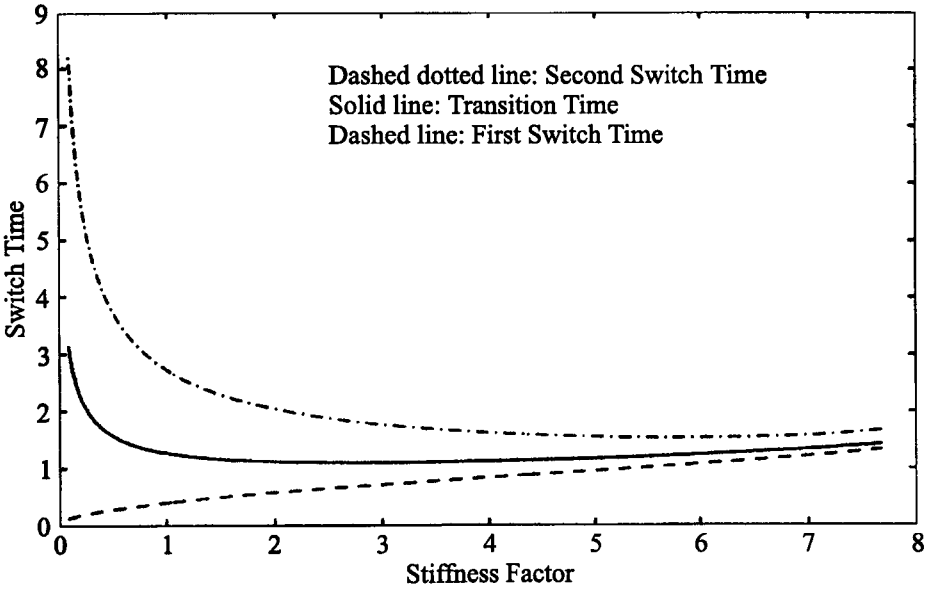

Figure 10. Variation of switch and transition time versus stiffness factor.

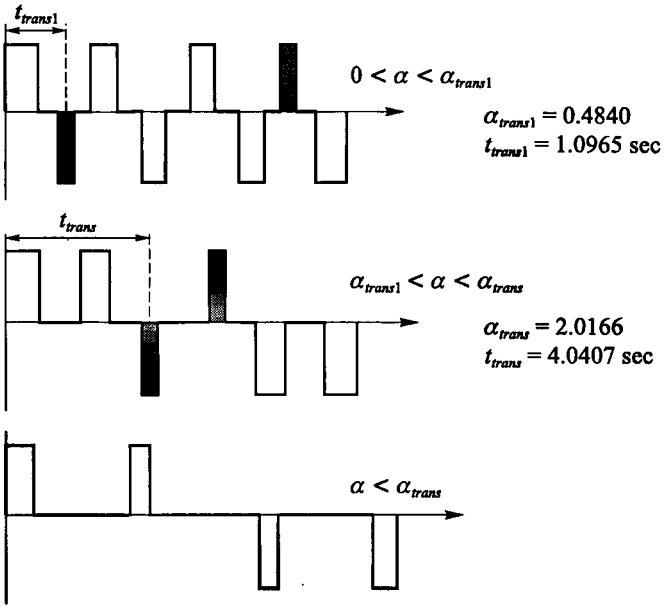

Figure 11. Transition profiles in the small α range for four-mass-spring system.

of the stiffness on α_{trans} and the transition switch point t_{trans} is shown in Figures 9 and 10, which were generated by the procedure delineated in the previous section.

As the stiffness increases, the value of the transition weighting parameter converges toward zero and increases rapidly with a decreasing stiffness factor lower than 1. Hence, paying attention to the existence of the small α profile (transition profile) becomes very important in a soft structure. Figure 10 also reveals that with the stiffness of the structure, the transition switch point for the additional pulse of the small α profile approximates the switch points of its neighbored switch times, indicating short off-periods and a small transition region for a fairly stiff system.

7.5. Transition Profile for Four-Mass-Spring System

The four-mass-spring system represents the class of structures that have more than one pair of fuel-wasting pulses in the small α profile. Increasing α in the valid range of the transition profile reveals that all the fuel-wasting pulses do not collapse simultaneously at α_{trans}, which denotes the value of complete transformation. The first decelerating pulse in the acceleration phase collapses at $\alpha_{trans1} < \alpha_{trans}$, leading to different transition profiles in the small α range $(0 < \alpha < \alpha_{trans})$. The two different transition profiles for the four-mass-spring system are shown in Figure 11.

The presence of different transition weighting parameters enables us to determine each transition point separately by the procedure presented above. The number of pulses P_s that vanishes with $\alpha > \alpha_{trans}$ is related to the number of flexible modes n and is given by

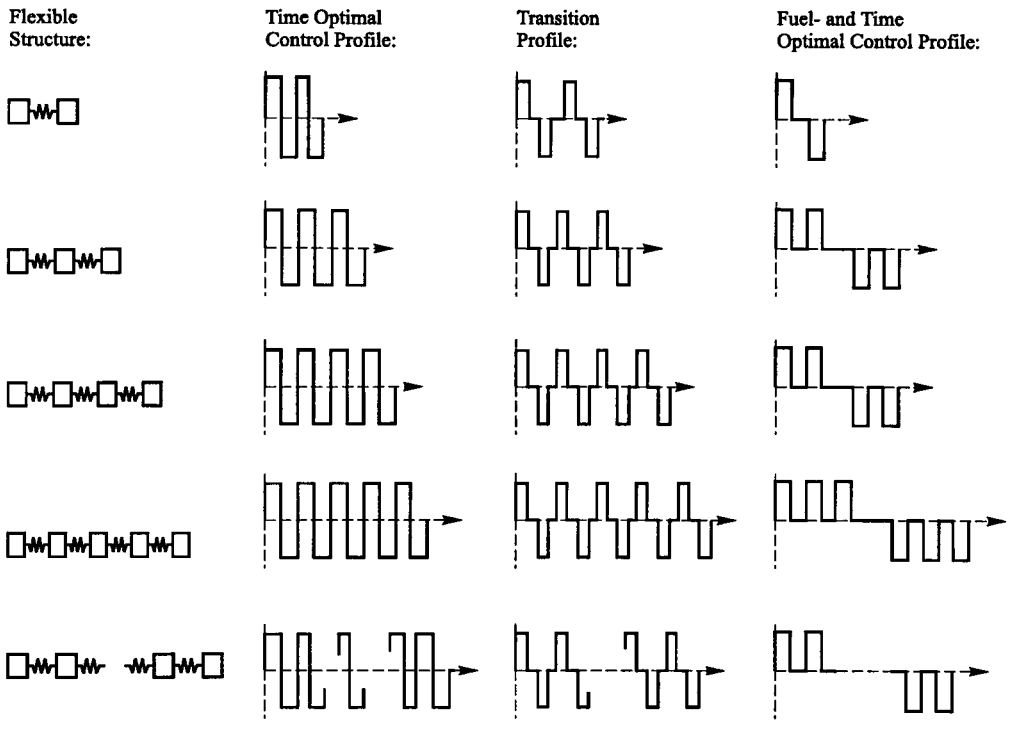

Figure 12. Time- and fuel/time optimal control profiles according to the number of flexible modes.

$$p_s = n+1, \text{ for } n = 1,3,5,\ldots \text{ (odd number of flexible modes)} \quad (56)$$

$$p_s = n, \text{ for } n = 2,4,6,\ldots \text{ (even number of flexible modes)} \quad (57)$$

Figure 12 gives an overview of the effects of number of vibratory modes of the structure to the optimal control profile.

8. CONCLUSIONS

A frequency domain approach to design fuel- and time-optimal controller for rest-to-rest maneuver of undamped flexible structures has been presented. It has been shown that the fuel- and time-optimal control consists of an on-off pulse sequence ("bang-off-bang" type). The optimal solution is dependent not only on the system boundary constraints but also on the number of flexible modes of the structure. The variation of the weighting parameter α penalizing the fuel consumption reveals two fundamental properties of the fuel- and time-optimal control:

1. Discontinuities in the switch times and final maneuver time as a function of the weighting parameter. Furthermore, for large values of α, the optimal solution is almost constant over a certain range of α.
2. The existence of transition profile(s) in the small α range, which, in its limits, is able to generate both time-optimal and fuel- and time-optimal control profiles. The small α profile is marked by decelerating pulses in the acceleration phase and accelerating pulses in the deceleration phase, which collapse completely at a certain value of α_{trans}.

The influence of the systems parameter on the solution in the transition region was examined. The knowledge about the transition region and its influencing factors is important, since it crucially determines the structure of the controller.

The complex constraints that permit multiple solutions lead to numerical difficulties in the optimization. Current research efforts are directed at extending the frequency domain approach to solve fuel/time optimal controller for damped system and to determine control profiles that are robust to errors in system parameters.

REFERENCES

Athans, M. and Falb, P., 1966, *Optimal Control: An Introduction to the Theory and Its Applications,* McGraw-Hill, New York.

Hartmann, R., 1994, "Robust fuel/time optimal control of flexible space structures: A frequency domain approach," M.S. thesis, Department of Mechanical and Aerospace Engineering, State University of New York at Buffalo, Buffalo, NY.

Kirk, D. E., 1970, *Optimal Control Theory: An Introduction,* Prentice Hall, Englewood Cliffs, NJ.

Lopes de Oliveira e Souza, M., 1988, "Exactly solving the weighted time/fuel optimal control of an undamped harmonic oscillator," *AIAA Journal of Guidance, Control, and Dynamics* **11**, 488-494.

Seywald, H., Kumar, R. R., Deshpande S. S., and Heck, M. L., 1994, "Minimum fuel spacecraft reorientation," *AIAA Journal of Guidance, Control, and Dynamics* **17**, 21-29.

Silverberg, L. and Redmond, J., 1993, "Fuel-optimal propulsive reboost of flexible spacecraft," *AIAA Journal of Guidance, Control, and Dynamics* **16**, 294-300.

Singh, G., Kabamba, P. T., and McClamroch, N. H., 1989, "Planar time-optimal control, rest-to-rest slewing of flexible spacecraft," *AIAA Journal of Guidance, Control, and Dynamics* **12**, 71-81.

Singh, T., 1995, "Fuel/time optimal control of the benchmark two-mass/spring system," *AIAA Journal of Guidance, Control, and Dynamics* **18**, 1225-1231.

Singh, T. and Vadali, S. R., 1994, "Robust time-optimal control: A frequency domain approach," *AIAA Journal of Guidance, Control, and Dynamics* **17**, 346-353.

Vander Velde, W. E. and He, J., 1983, "Design of space structure control systems using on-off thrusters," *AIAA Journal of Guidance, Control, and Dynamics* **6**, 53-60.

Wie, B., Sinha, R., Sunkel, J., and Cox, K., 1993, "Robust fuel- and time-optimal control of uncertain flexible space structures," in *Proceedings of the AIAA Guidance, Navigation and Control Conference,* Monterey, CA, pp. 939-948.